Original Research Article

Structural Shear behavior of Composite Box beams using advanced innovated materials

ABSTRACT

This paper opens a new conception of shear behaviour of box concrete beams reinforced by composite fabrics. For this purpose, stirrups, wire meshes as shear reinforcement were used. Seven box section concrete beams were tested using two-point loading system. Beams with tensar wire mesh exhibited increasing in ultimate failure load, shear capacity and deflection with respect to beams with reference & fiber-glass wire mesh. Nonlinear finite element analysis was conducted using ANSYS 14.5 to verify the experimental test program. Good agreement was found between the experimental and numerical results.

Keywords: [Composite structures, box beams, shear stress, composite materials, glass fiber wire mesh, tensar wire mesh, nonlinear finite element analysis (NLFEA), Ansys 14.5}

1. INTRODUCTION

Wire meshes were used to belay the new system and to improve its performance [1,2]. Ferrocement is named as wire mesh reinforcement. The flexure behavior of wire meshes had been studied and noticed to be nearly to reinforced concrete members [3,6]
A1-Sulaimani et al [7,8] recommended studying the behavior of composite ferrocement beams under transversal shear stress. Mansur & Ong [9] had studied the shear behaviour of rectangular ferrocement beams. Ferrocement rectangular beams were found to be critical to shear collapse at comparatively high Vf and f'c. El-Sayed & Erfan [10] improved the shear behaviour of ferrocement composite beams. Test results showed that beams with expanded wire mesh exhibited some amount of increase in shear capacity with respect to beams with reference & welded wire mesh.

2. EXPERIMENTAL PROGRAM

The experimental work was done to investigate the general behaviour, cracks pattern, shear stresses and the ultimate capacity of the reinforced concrete box beam reinforced by composite fabrics. The experimental program consisted of seven composite box beams having the cross- sectional dimensions of 100 mm x200 mm and 1800 mm long were cast and tested until failure. All specimens were reinforced with the same longitudinal bars in tension and compression. The specimens were tested using two-point loading. The reinforcing bars were designed and detailed, and the bearing pad was proportioned such that the flexural, anchorage and bearing modes of failure were avoided. The concrete mix for the test specimens was designed to obtain compressive strength at 28 days of 30 MPa. The mix proportions were 2 sand: 1 cement, water cement ratio was 0.3 and 1.5% super plasticizer by weight of cement. The concrete slump was found to be 130 mm and a density of 2500 Kg/m^3. All specimens were tested using compression testing machine of capacity 2000 KN.

2.1 Preparation of Specimens and samples description

The experimental program consists of seven box beams with the same geometry and steel reinforcement details as shown in Fig. 1, were prepared for testing under concentric loads. The control specimen was box section beam reinforced using 2Ø12 in tensions and 2Ø10 in compression and 13Ø6 as stirrups. The other sixth box beams haven't stirrups but using glass fiber and tensar composite instead of stirrups. The first group consists of three beams Box1-1, Box2-1 and Box3-1 which reinforced using one, two and three layers of glass fiber wire mesh respectively. Second group for Box1-2, Box2-2 and Box3-2 which reinforced using one, two and three tensar wire mesh instead of stirrups respectively as described in Table 1.

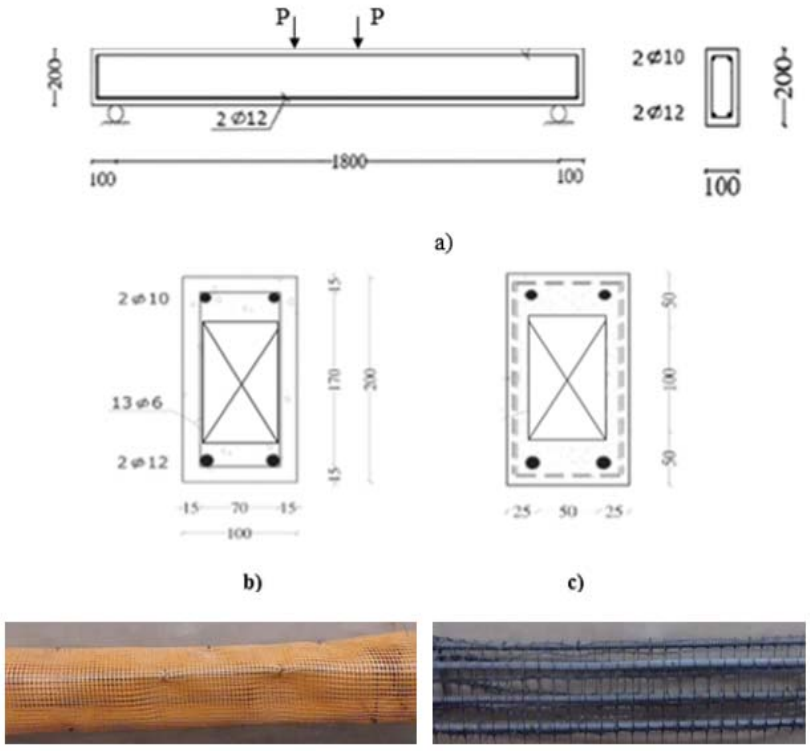

Fig.1: beams geometric shape and reinforcement details, a) Control specimen; b) Cross-section of beam with steel stirrups; c) Cross-section of beam glass fiber wire mesh or tensar layer mesh; d) Beams with glass fiber wire mesh; e) Beams with tensar wire mesh

Table 1: Box beams specimen's descriptions and notations

Series	Specimen No.	Specimens description	Reinf. Tension	Compression	Vr. Stirrups
Control	**BOX1**	**Control specimen**	**2φ12**	**2 φ10**	**13Φ6**
Group 1 "Glass fiber wire Mesh"	**BOX1-1**	**One-layer glass fiber**	**2 φ12**	**2 φ10**	**-**
	BOX2-1	**Two-layer glass fiber**	**2 φ12**	**2 φ10**	**-**
	BOX3-1	**Three-layer glass**	**2 φ12**	**2 φ10**	**-**

		fiber			
Group 2 "Tensar wire mesh"	**BOX1-2**	**One-layer tensar**	**2φ12**	**2 φ10**	**-**
	BOX2-2	**Two-layer tensar**	**2 φ12**	**2 φ10**	**-**
	BOX3-2	**Three-layer tensar**	**2 φ12**	**2 φ10**	**-**

2.2 Characteristics of Materials

The concrete mix contents utilized for the experimental program was summarized in Table 2 which gives concrete characteristic strength of 30 MPa. The reinforced steel obtained from El-Dekhiela factory was fy=360 MPa (for deformed bars) and fy=240 MPa (for plain bars). Fig.2 showed either tensar or fiber glass wire meshed used. Table 3 summarized the properties of both wire meshes as per manufacturer. The beams were casted in a horizontal position and the vibrated concrete placed compacted in wooden molds.

Table 2: The Contents of Concrete Mixture

Contents	Amount
Cement	350 K_g/m^3
Sand	700 K_g/m^3
Aggregate (1)	540 K_g/m^3
Aggregate (2)	620 K_g/m^3
Water	162.5 L/m^3
Admix	2 L/m^3

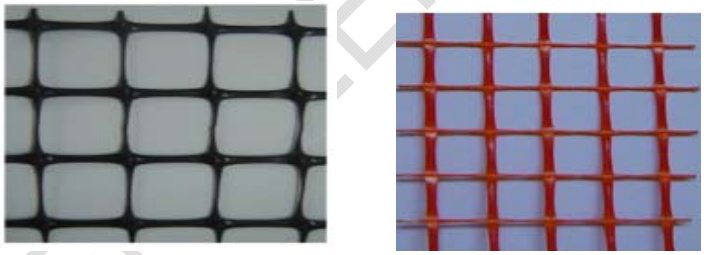

a) **b)**

Fig.2: Configurations of composites materials; a) Polyethylene (Tensar) wire mesh, b) Fiber glass wire mesh

Table 3: Mechanical properties of tensar and fiber glss wire meshes

Polyethylene (Tensar) wire mesh		Glass fiber wire mesh	
Dimensions size	6.0 x 8.0 mm	Dimensions size	12.5 x 11.5 mm
Weight	725 gm/m^2	Weight	123 gm/m^2
Sheet Thickness	3.30 mm	Sheet Thickness	0.66 mm
Yield Stress	260 N/mm^2	Yield Stress	230 N/mm^2
Young's modulus	100000	Young's modulus	80000

2.3 Test setup

The composite box beams were tested under two-point load testing machine of maximum capacity of 2000 KN with 1800mm effective span and 750mm shear span and 300mm load distance as shown in Fig. 3. Load was affective at 20 KN increments on the tested specimens. The LVDT and dial gages were used of high accuracy to measure the deflections and strains for steel and concrete. The load still increased till failure load and maximum displacements.

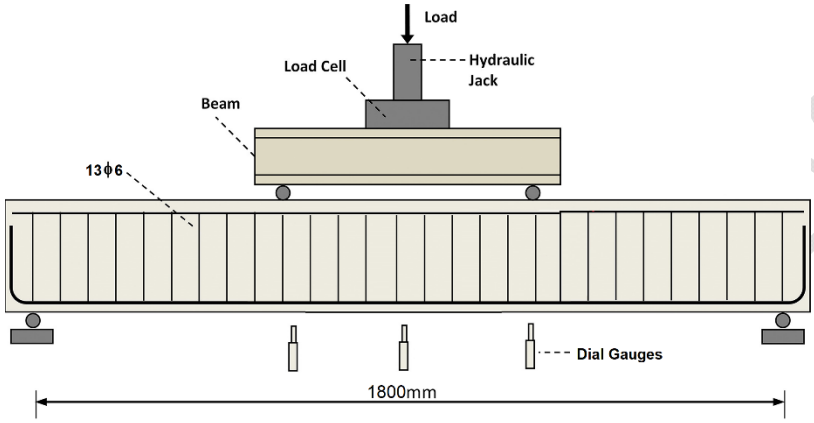

Fig. 3: Test set up schematic

3. RESULTS AND DISCUSSION

Test results include the load carrying capacity and displacement in concrete box beams. The cracks propagation during the tests was recorded. The crack initialization in the specimens reinforced using wire meshes was developed however, at later stages with respect to the control specimen. Also, the cracks lengths and widths decreased in the specimens reinforced with either glass fiber or tensar wire meshes as compared with the control specimen.

3.1 Cracking

The first crack for all tested box beams were developed horizontally under the load pint in the mid span. Control specimen cracks observed at a load of 7.5 KN. For specimens BOX1-1, BOX2-1 and BOX3-1, a higher ultimate load was recorded 1.04, 1.1 and 1.25 times than control one respectively. The diagonal cracking initiated in the Control Specimen; BOX1 increased in length and width until failure at load of 42.5 KN. For specimens BOX1-2, BOX2-2 and BOX3-2, a higher ultimate load was recorded 1.02, 1.12 and 1.18 times than control specimen respectively. Using fiber glass wire mesh and tensar wire mesh instead of stirrups was enhanced the crack pattern for box beams as shown in Fig. 4.

a)

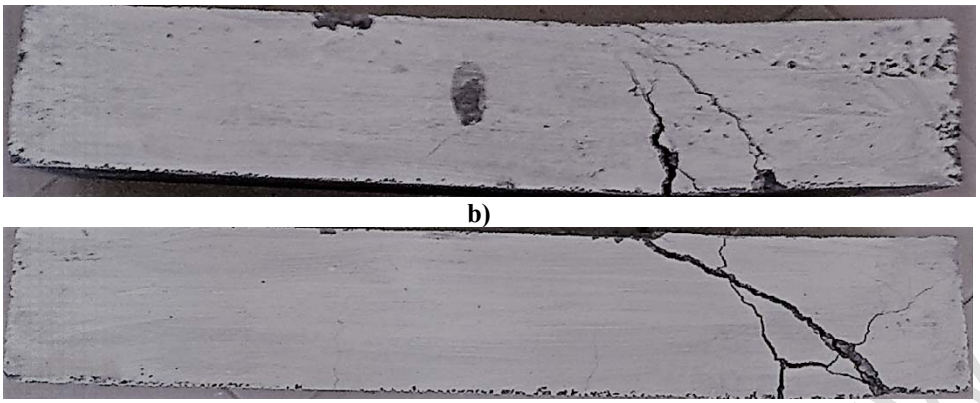

b)

c)

Fig.4: Sample of crack pattern; a) control specimen; b) glass fiber wire mesh; c) Polyethylene (tensar) wire mesh.

3.2 Ultimate load Capacity

The load carrying capacity is differ from one box beam to another according to its reinforcement and using tensar and glass fiber wire mesh instead of steel stirrups. For the control specimen, the ultimate failure load was 40.5 KN. The first group which reinforced using glass fiber wire mesh recorded failure loads of 45.7, 47.3 and 50.2 KN for BOX1-1, BOX2-1 and BOX3-1 respectively with enhancement ratio with respect to the control beam of 12.8, 16.8 and 23.9% respectively. This enhancement related to layers number of glass fiber wire mesh used in reinforcement as shown in Table 4. For the second group which reinforced using Polyethylene (tensar) wire mesh of different layers number of BOX1-2, BOX2-2 and BOX3-2. The experimental failure loads were 48.44, 51.6 and 55.2 KN with enhancement ratio of 19.6, 27.4 and 36.3% for BOX1-2, BOX2-2 and BOX3-2 respectively. Observing that using three layers of either glass fiber or tensar wire mesh recorded the highest load and enhancement in carrying capacity. It is noticed that the effect of using tensar wire mesh has the major effect in load carrying capacity as shown in Table 4 and Fig. 5.

Table 4: Experimental testing results

Series	Specimen No.	Failure load (KN)	% Of enhancement in load	Deflection (mm) at failure load
Control	BOX1	40.5	----	0.40
Group 1 "glass fiber wire mesh"	BOX1-1	45.7	12.8	0.290
	BOX2-1	47.3	16.8	0.278
	BOX3-1	50.2	23.9	0.250
Group 2 "Polyethylene (tensar)wire mesh"	BOX1-2	48.4	19.6	0.270
	BOX2-2	51.6	27.4	0.250
	BOX3-2	55.2	36.3	0.230

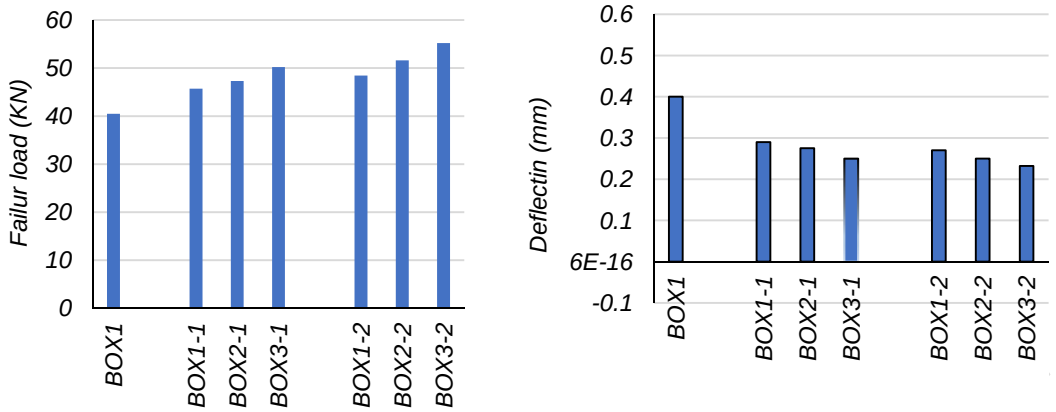

a) b)

Fig. 5: comparison between experimental results; a) failure load (KN); b) deflection (mm) at ultimate load of control specimen

3.3 Experimental ultimate deflection

As shown in Table 4 and Figs. 5.b and 6 the experimental deflection recorded for different specimens with different reinforcement types. The deflection recorded for the control specimen was 0.40 mm at failure load. For group one which reinforced with glass fiber wire mesh, the maximum deflection at failure load was 0.38, 0.39 and 0.45 mm but at the same failure load of the control, it was 0.29, 0.278 and 0.25 mm respectively which is lower than the control specimen. This indicates the effect of glass fiber wire mesh in decreasing the deflection with average ratio of 32%. For group two which reinforced with Polyethylene (tensar) wire mesh, the maximum deflection at failure load was 0.41, 0.44 and 0.45 mm which is higher than the control specimen but if the deflection recorded at specimens BOX1-2, BOX2-2 and BOX3-2 at failure load of control specimen which was 0.27, 0.25 and 0.23 mm respectively. This indicates the effect of tensar wire mesh in decreasing the deflection with average ratio of 37.5%. This ratio indicates that the tensar wire mesh has the best effect in decrease the deflection.

The decrease in ultimate deflection of group one and two is mainly due to increase in number of glass fiber or tensar wire mesh layers used in reinforcement instead of steel stirrups which lead to increase in its volume fraction in specimens.

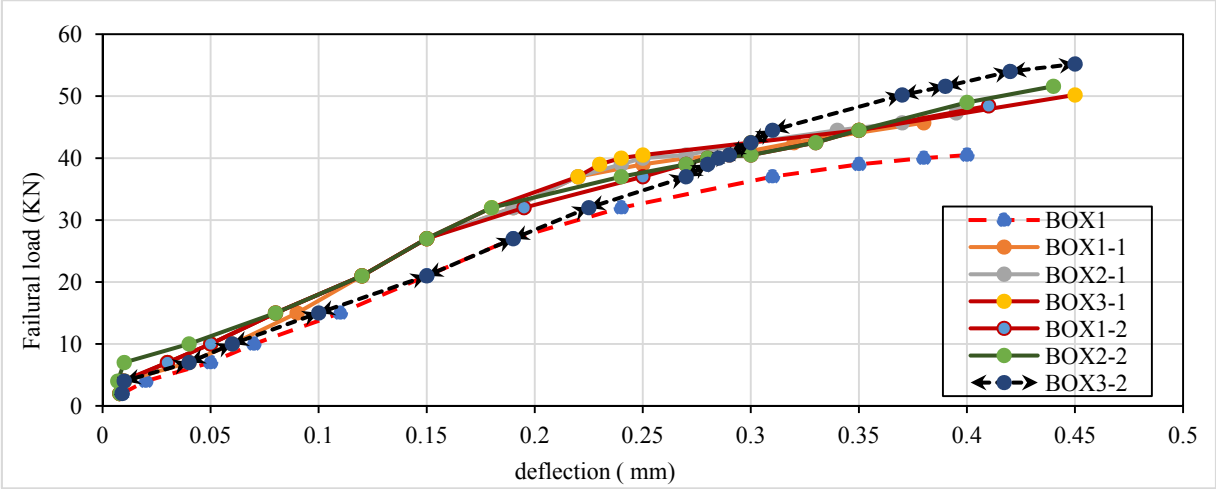

Fig. 6: Experimental load deflection curve

3.4 Ductility and energy absorption

Ductility is defined as the ratio between the deflections at ultimate load to the deflection at the first crack load but the energy absorption is the total area under the load deflection curve. The ductility recorded an average ratio for different specimens of 5.66. A progressive increase of energy absorption which represents the specimen toughness with volume friction percentage and ductility was observed. For the control specimen BOX1 the energy absorption recorded 285.6 KN.mm, compared this value with the recorded for different series it shows good enhancement. For all series the enhancement percentage varies between 99.6% and 129%. The smallest enhancement was at specimen BOX1-2 which use one glass fiber layer instead of stirrups due to the weak properties of the used type of layer but the highest enhancement was in BOX3-2 which used three tensar layers wire mesh. Finally using reinforced with various types of composite materials were developed with high ultimate loads, crack resistance, better deformation characteristics, high durability and energy absorption properties, which are very useful for dynamic effect.

3.5 shear stress

The obtained shear stresses are obtained according to the ECP203/207 [11]. For the control specimen BOX1 the shear stress was 2.25 MPa. For the first group box beams BOX1-1, BOX2-1 and BOX3-1 the shear stresses were 2.53, 2.62 and 2.78 MPa respectively with an enhancement ratio of 12.5%, 16.5% and 23.5% respectively with respect to the control specimen. The second group which used Polyethylene (tensar) wire mesh instead of stirrups, the shear stresses was 2.69MPa, 2.86 MPa and 3.06 MPa for BOX1-2, BOX2-2 and BOX3-2 respectively. The enhancement in this group with respect to the control specimen was 19.5%, 27.1% and 36.0% respectively which is relatively more than the group used the glass fiber wire mesh.

4. Non-linear finite element analysis study

NLFEA study was done to verify the obtained experimental results. The groups studied were as shown in Table 1 which divided in to control specimen and other two groups. Group one which used glass fiber wire mesh instead of steel stirrups with different number of layers. The second group used Polyethylene (tensar) wire mesh instead of steel stirrups. These specimens were modeled and analyzed using ANSYS 14.5 [12] program.

4.1 specimens modeling

NLFEA was carried out to estimate the behavior of composite box beams as shown in Fig. 7. The discussed behavior included the ultimate capacity, deflection, shear stresses and crack pattern for each specimen.

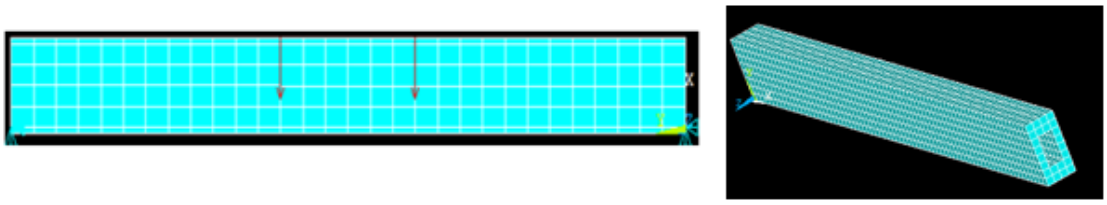

a) Model of box beam under loads b) model of box beam

Fig. 7: NLFEA model of examined box beams

4.1.1 Model Elements Types

Solid 65 represent the concrete element which represents the stress strain curve for concrete in compression and the other properties of it represent the concrete strength in tension. The other used element was LINK 8 3-D to represent the steel bars with its strength and steel stirrups. The composite materials of glass fiber or Polyethylene (tensar) wire mesh was represented by calculating the volumetric ratio of it in the concrete element using its properties by calculating the ratio of steel to concrete in each element as shown in Fig. 8. Each material has its X, Y and Z coordinates and has its orientation angle and its reinforcement in wire mesh smeared element.

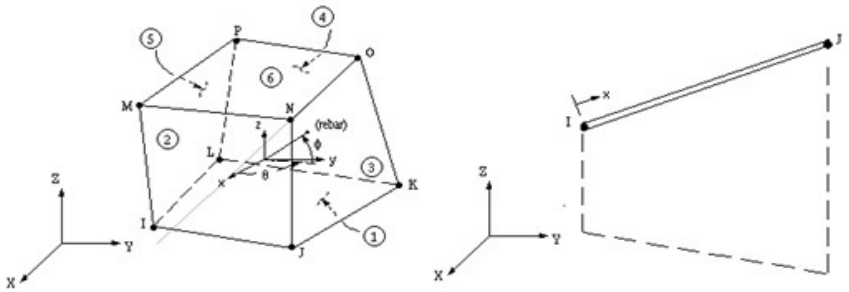

a) Solid65 b) Link8

Fig. 8: Geometry of element types

4.1.2 Modelling Material properties

The mechanical properties for element SOLID65 and LINK 8 which represent concrete and steel reinforcement respectively was Elastic modulus of elasticity (E_c= 4400$\sqrt{f_{cu}}$=24100 N/mm^2) and Poisson's ratio (v= 0.3), but Yield stress (f_y= 360 N/mm^2 & f_{yst}= 240 N/mm^2) with Poisson's ratio v= 0.2, [11].

For the element which represents the composite properties for glass fiber wire mesh are as the given. The glass fiber wire mesh which has diamond size is 12.5 x 11.5mm with thickness of 0.66 mm, the volumetric ratio of one layer of glass fiber mesh (V1= 0.00872), two layers was (V1= 0.0174) but for the three layers of glass fiber the volumetric ratio is (V1= 0.02616). For the Polyethylene (tensar) layers the size of opening is 6.0 x8.0mm with wires of diameter 3.3 mm. The volumetric ratio of one layer of tensar mesh (V1= 0.14800), two layers was (V1= 0.29600) but for the three layers the volumetric ratio of three layer of tensar mesh (V1= 0.44400).

4.2 Analytical Results and Discussion

The finite element program presents the nonlinear response of the box beams specimens. Loading was incrementally increased until failure and divergence occurs which lead to failure. The finite element results represent the cracks patterns, failure load, deflection, shear stresses and yielding of steel as shown in Table 5.

4.2.1 Cracking

The first crack in the entire tested box beam was slightly inclined crack developed under the load pint in the mid span. This first crack in the control specimen observed at a load of 4.0 KN. For specimens BOX1-1, BOX2-1 and BOX3-1, it was recorded at a higher load being 1.2, 1.15 and 1.05 times that of the Control Specimen; BOX1, respectively. The cracking initiated in the Control Specimen; BOX1 increased in numbers until failure at load of 36 KN. For specimens BOX1-2, BOX2-2 and BOX3-2, it was recorded at a higher load with respect to control specimen being 0.95, 1.05 and 1.12 times that of the control specimen; BOX1, respectively. Using the fiber glass wire mesh and Polyethylene (tensar) wire mesh instead of stirrups enhance the crack pattern for box section beam as shown in Fig. 9C.

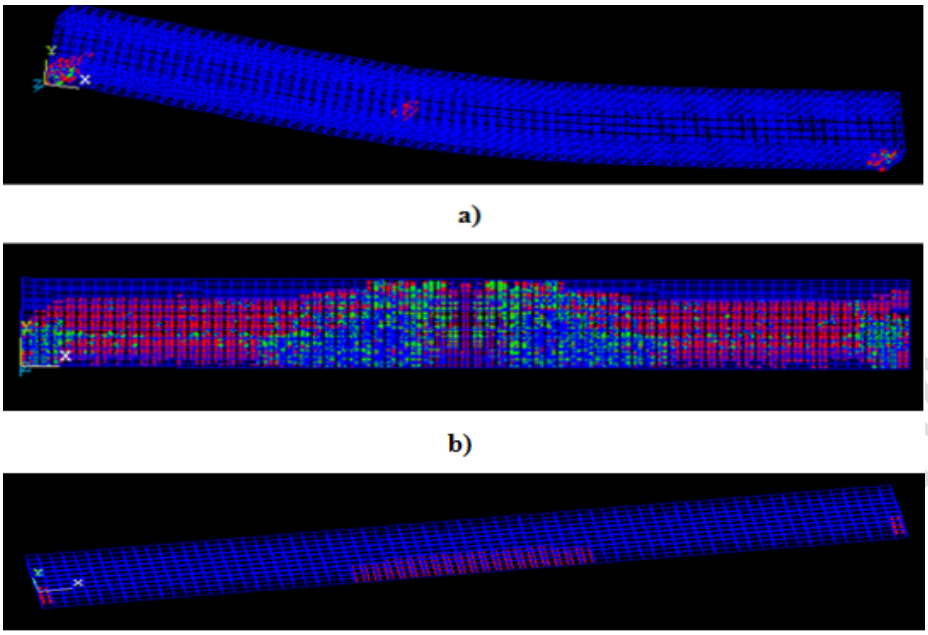

Fig.9: Sample of crack pattern for control specimen; a) first cracks; b) cracks at failure; c) sample of cracks for specimens in group 1 and 2.

4.2.2 Ultimate Failure Load

The load carrying capacity is differing from one box section to another according to its reinforcement and using glass fiber wire mesh and polyethylene (tenasr) wire mesh instead of steel stirrups. For the control specimen BOX, the ultimate failure load was 36.0 KN. The first group which reinforced using glass fiber wire mesh recorded failure loads of 42.8, 44.2 and 48.3 KN for BOX1-1, BOX2-1 and BOX3-1 respectively with enhancement ratio with respect to the control beam of 18.8%, 22.8% and 34.1% respectively. This enhancement related to number of fiber glass wire mesh used in reinforcement as shown in Table 5. For the second group which reinforced using tensar wire mesh of different layers number of BOX1-2, BOX2-2 and BOX3-2. The NLFE failure loads were 45.7, 49.2 and 53.4 KN with enhancement ratio of 26.9%, 36.7% and 48.3% for BOX1-2, BOX2-2 and BOX3-2 respectively. Observing that using three layers of either glass fiber or tensar wire mesh recorded the highest load and enhancement in carrying capacity. It is noticed that the effect of using tensar wire mesh has the major effect in load carrying capacity as shown in Table 5 and Fig. 10.

4.2.3 Analytical Ultimate deflection

The analytical deflection recorded for different specimens with different reinforcement types is recorded as in Table 5 and Fig. 10 and Fig. 11. The deflection of the control specimen was 0.37 mm at failure load. For group one which reinforced with glass fiber wire mesh, the maximum deflection at failure load was 0.35, 0.37 and 0.42 mm but at the same load of the control specimen it was 0.26, 0.24 and 0.25mm respectively which is lower than the control specimen. This indicates the effect of glass fiber wire mesh in decreasing the deflection with average ratio of 29.7%.

For group two which reinforced with Polyethylene (tensar) wire mesh, the maximum deflection at failure load was 0.40, 0.42 and 0.415 mm which is higher than the control specimen but if the deflection recorded at specimens BOX1-2, BOX2-2 andBOX3-2 at failure load of control specimen which was 0.265, 0.25 and 0.27 mm respectively. This indicates the effect of tensar wire mesh in decreasing the deflection with average ratio of 29.8%. This ratio indicates that the tensar wire mesh has relatively best effect in decrease the deflection.

The decrease in ultimate deflection of group one and two is mainly due to increase in number of glass fiber or tensar wire mesh layers used in reinforcement which lead to increase in its volume fraction in specimens.

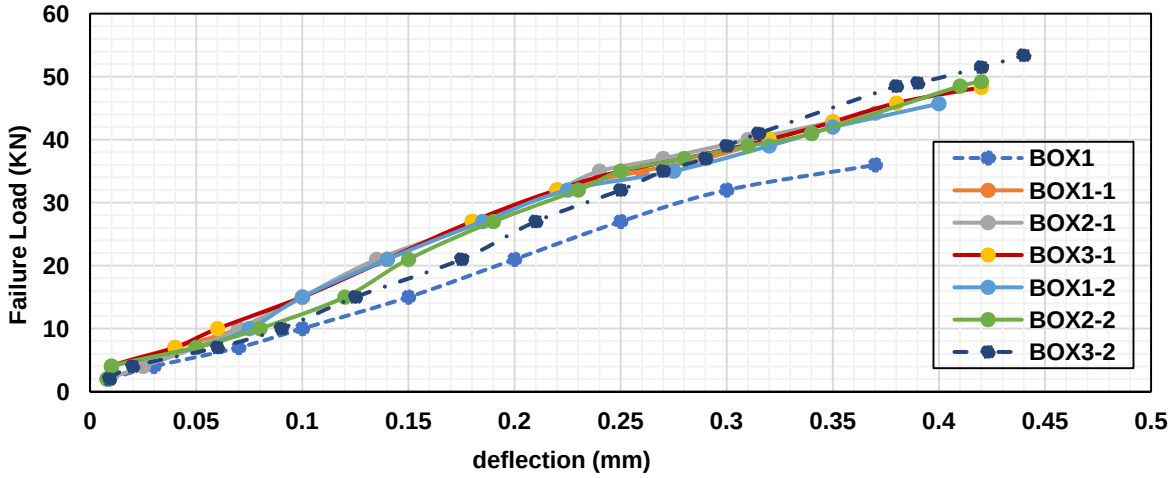

Fig. 10: NLFE load deflection curves

Table 5: NLFEA Analytical Results

Series	Specimen No.	Failure load (KN)	% Of enhancement in load	Deflection (mm) at failure load
Control	BOX1	36.0	---	0.370
Group 1 "glass fiber wire mesh"	BOX1-1	42.8	18.8	0.370
	BOX2-1	44.2	22.8	0.350
	BOX3-1	48.3	34.1	0.420
Group 2 "Polyethylene (tensar) wire mesh"	BOX1-2	45.7	26.9	0.400
	BOX2-2	49.2	36.7	0.410
	BOX3-2	53.4	48.3	0.415

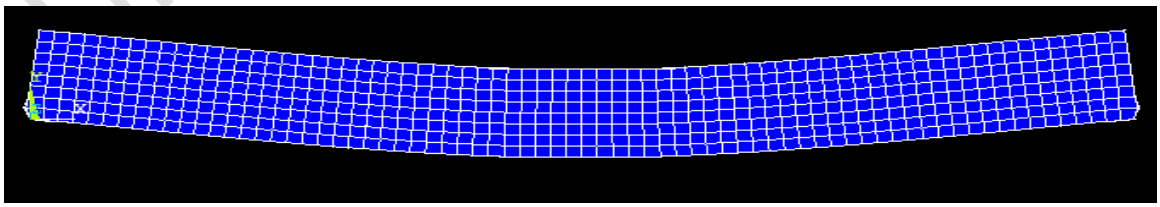

Fig.11 Typical deformation of NLFEA deflection for box beams

4.2.4 Ductility and energy absorption

A progressive increase of energy absorption which represents the specimen toughness with volume friction percentage and ductility was observed. For the control specimen BOX1 the energy absorption recorded 249.9 KN.mm, compared this value with the recorded for different series it shows good enhancement. For all series the enhancement percentage varies between 45.1% and 159%. The smallest enhancement was at specimen BOX1-2 which use one Polyethylene (tensar) layer instead of stirrups due to the properties of the used type of layer but the highest enhancement was in BOX3-1 which used three tensar layers wire mesh which agreed with the results. Finally using composite materials were developed with high ultimate loads, crack resistance, better deformation characteristics, high durability and energy absorption properties, which are very useful for dynamic effect.

4.2.5 Shear Stresses

The obtained shear stresses are obtained according to the obtained results from the NLFEA as shown in Fig.12. For the control specimen BOX1 the shear stress was 2.0 MPa. For the first group box beams BOX1-1, BOX2-1 and BOX3-1 the shear stresses were 2.37, 2.45 and 2.68 MPa respectively with an enhancement ratio of 18.5%, 22.5% and 34.0% respectively with respect to the control specimen. The second group which used the Polyethylene (tensar) wire mesh instead of stirrups, the shear stresses was 2.53 MPa, 2.73 MPa and 2.96 MPa for BOX1-2, BOX2-2 and BOX3-2 respectively. The enhancement in this group with respect to the control specimen was 26.5%, 36.5% and 48.0% respectively which is relatively more than the group used the glass fiber wire mesh.

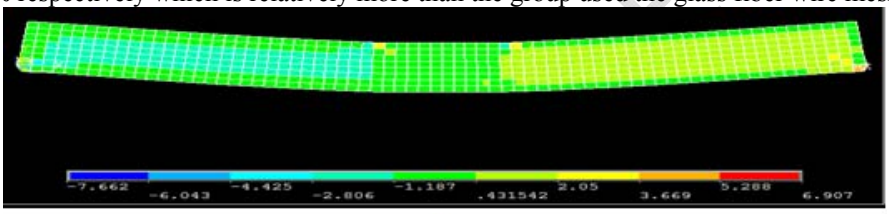

a)

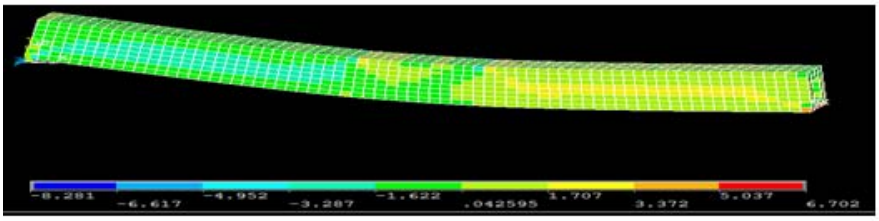

b)

Fig.12 NLFEA Shear Stresses; a) Shear stresses for BOX1; b) Sample of shear stresses for different specimens

5. Comparison between experimental and NLFEA results

These comparisons aim to ensure the NLFEA models are available and suitable to exhibit the response of composite box beams. There are seven finite element models were compared with seven experimental specimens in term of ultimate load, ultimate deflection and crack patterns.

5.1 Ultimate failure load

There was an acceptable agreement between the experimental failure load and the analytical failure load obtained from NLFE program as shown in Table 6 and Fig.13. The ratio between the NLFE

failure loads to the experimental failure load varies between 0.90 to 0.96 with an average ratio of 0.94. The ratio of $P_{u\ NLFE}$/ $P_{u\ Exp}$ for control specimen was 0.90 but for the specimens in group one, it was 0.93, 0.94 and 0.96 for BOX 1-1, BOX2-1 and BOX3-1 respectively.
For the second group this ratio was 0.94, 0.95 and 0.96 for BOX 1-2, BOX2-2 and BOX3-2 respectively. This shows that the NLFEA gives the aim of the studied parameters in face of load carrying capacity.

5.2 Ultimate Deflection

Fig. 14 showed the load deflection curves for all box beams in phase of experimental and NLFE obtained results. The recorded deflection for experimental and NLFE analysis showed an agreement with respect to the deflection recorded for the control specimen as in Figure 15 and Table 6. The recorded ratio between Δ_{NLFE} / Δ_{Exp} of 0.92 for the control specimen. For the first group this ratio recorded 0.92, 0.95 and 0.93 for BOX 1-1, BOX2-1 and BOX3-1 respectively but for BOX 1-2, BOX2-2 and BOX3-2, these ratios were 0.97, 0.95 and 0.92 respectively. These ratios showed that NLFE program provide an acceptable response in deflection as in Fig. 15.

Table 6: Comparison between experimental and NLFE Analysis

specimen	Failure load P_{ult} (KN)		Deflection Δ_{ult} (mm)		Shear stress Vu (MPa)		P_{ult} NLFEA/ P_{ult} exp	Δ_{ult} NLFE/ $\Delta_{ult\ t}$ exp	V_u NLFEA/ V_u exp
	NLFEA	EXP	NLFEA	EXP	NLFEA	EXP			
BOX1	**36.0**	**40.5**	**0.37**	**0.40**	**2.0**	**2.25**	**0.90**	**0.92**	**0.89**
BOX1-1	**42.8**	**45.7**	**0.35**	**0.38**	**2.37**	**2.53**	**0.93**	**0.92**	**0.94**
BOX2-1	**44.2**	**47.3**	**0.37**	**0.39**	**2.45**	**2.62**	**0.94**	**0.95**	**0.93**
BOX3-1	**48.3**	**50.2**	**0.42**	**0.45**	**2.68**	**2.78**	**0.96**	**0.93**	**0.96**
BOX1-2	**45.7**	**48.4**	**0.40**	**0.41**	**2.53**	**2.69**	**0.94**	**0.97**	**0.94**
BOX2-2	**49.2**	**51.6**	**0.42**	**0.44**	**2.73**	**2.86**	**0.95**	**0.95**	**0.95**
BOX3-2	**53.4**	**55.2**	**0.415**	**0.45**	**2.96**	**3.06**	**0.96**	**0.92**	**0.96**

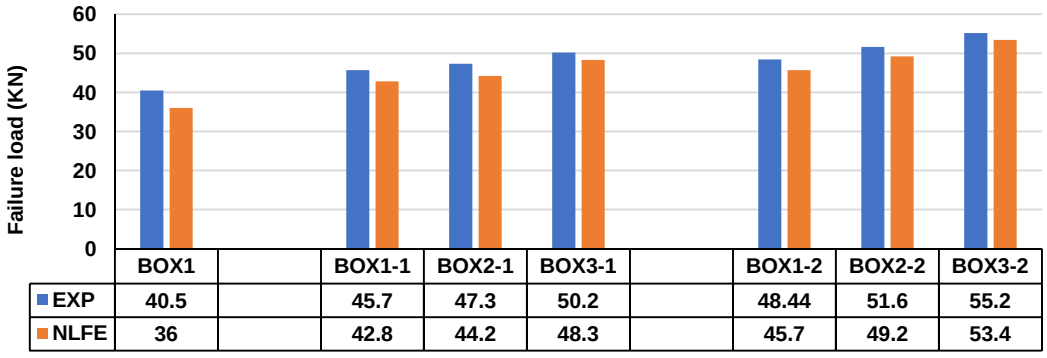

Fig. 13: Comparison between Exp. Failure load and NLFE failure load

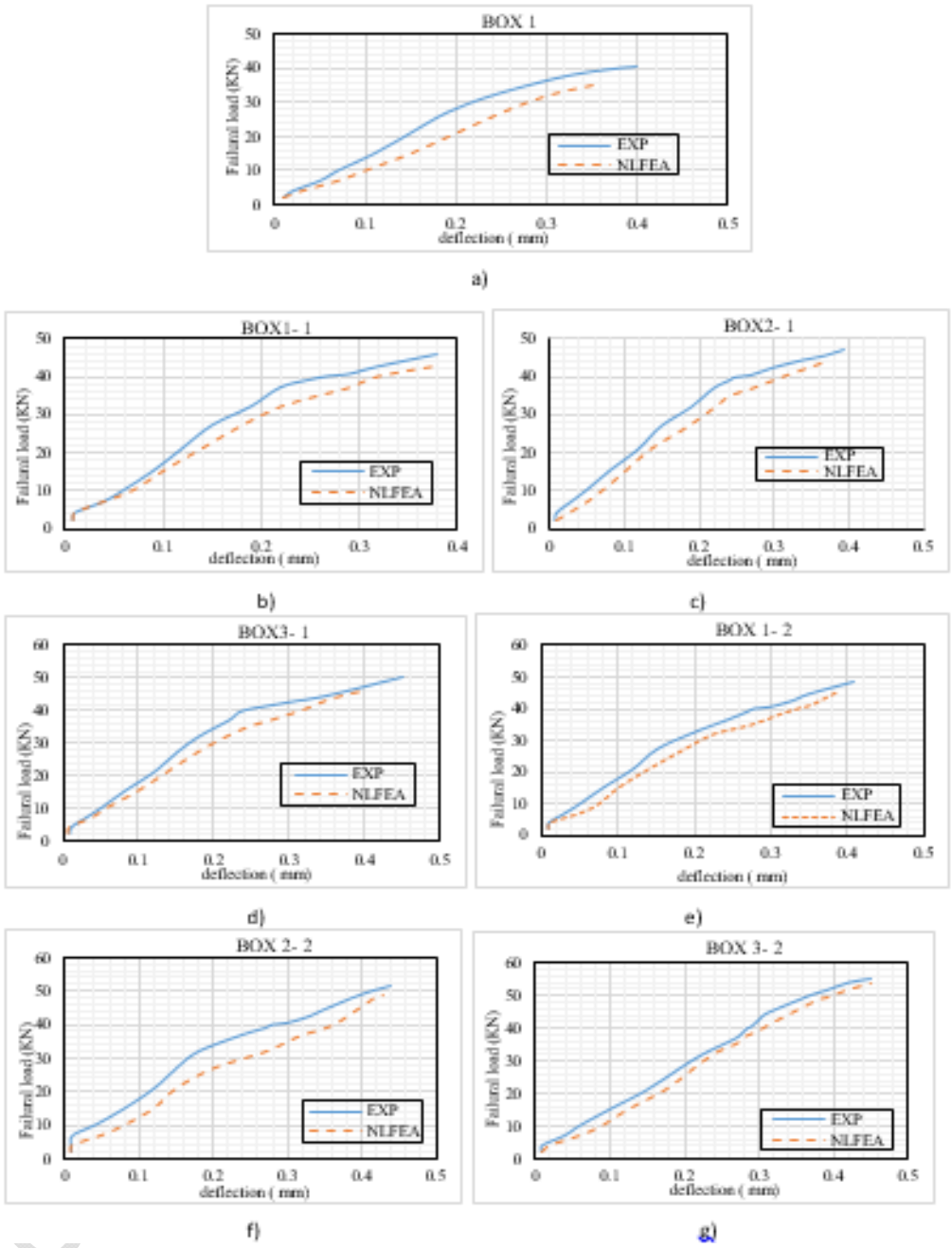

Fig. 14: Comparison between experimental and NLFEA load deflection curve; a) Control BOX1; b) BOX1-1; c) BOX2-1; d) BOX3-1; e) BOX1-2; f) BOX2-2; g) BOX3-1.

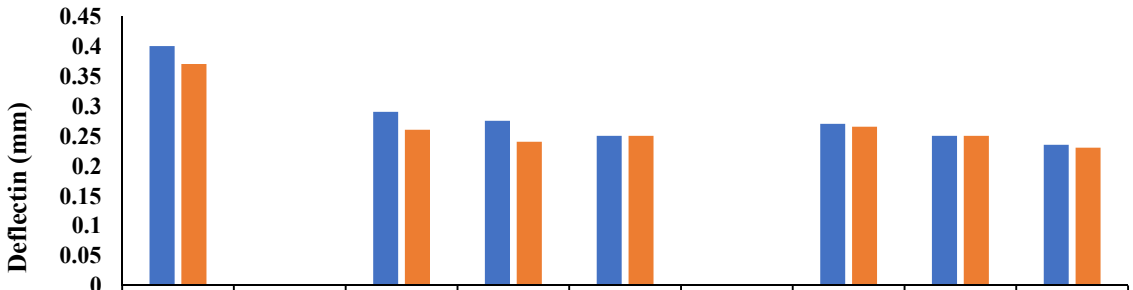

Fig.15: Comparison between Exp. deflection and NLFE deflection at the failure load of control specimen.

5.3 Crack Patterns

The Fig. 16 indicate a comparison between the crack patterns experimentally and in NLFE analysis these cracks begins micro cracks and increased in length and width till failure

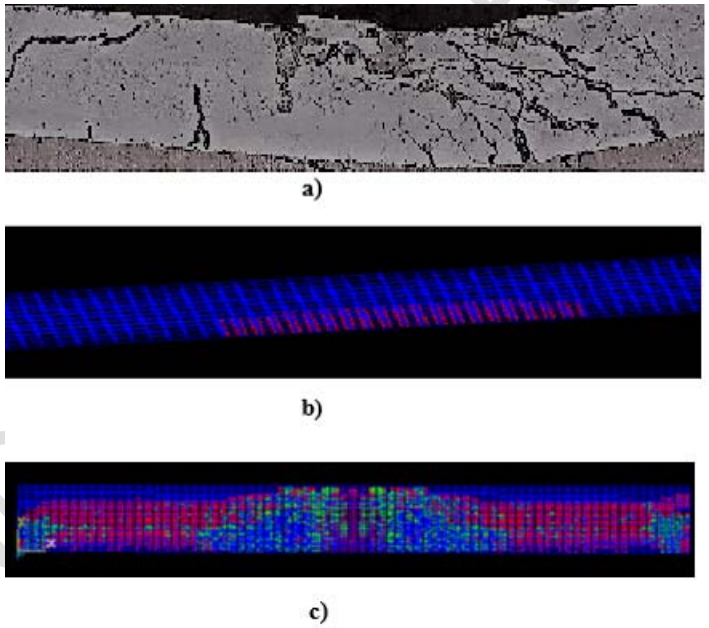

Fig.16: Crack pattern for box beams; a) Experimental crack pattern; b) NLFE crack pattern; c) NLFE cracks till failure.

5.4 Shear Stresses

As the porpouse of this study was to discuss the shear stresses and the effect of using wire meshes in resist shear and cracks propagates. The experimental and NLFEA showed reasonable agreement in the obtained results as shown in Fig. 17 and Table 6. The ratio between the shear stresses from NLFEA and experimental test was 0.89 for control specimen, but for the group one which used glass fiber wire mesh instead of steel stirrups this ratios was 0.94, 0.93 and 0.96 for BOX 1-1, BOX2-1 and BOX3-1

respectively. For the second group which used tensar wire mesh, the ratios were 0.94, 0.95 and 0.96 for BOX 1-2, BOX2-2 and BOX3-2 respectively. So, the finite element analysis represents an acceptable presentation for shear stresses.

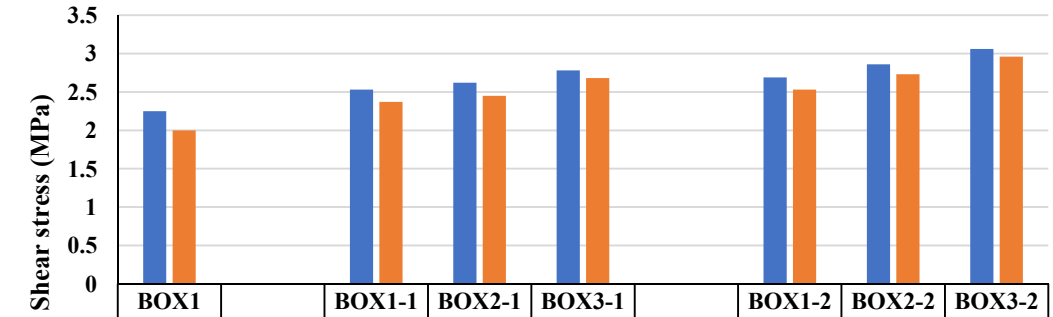

	BOX1		BOX1-1	BOX2-1	BOX3-1		BOX1-2	BOX2-2	BOX3-2
EXP.	2.25		2.53	2.62	2.78		2.69	2.86	3.06
NLFEA	2		2.37	2.45	2.68		2.53	2.73	2.96

Fig.17: Comparison between Exp. Shear stresses and NLFE Shear stresses.

6. CONCLUSIONS

The following conclusions can be drawn:

1- Glass fiber wire mesh and Polyethylene (tensar) wire mesh exhibited features over normal reinforcement with reinforcing steel, especially in box beams such that, it has high strength, easy to be handling cutting and shaped also has light weight with respect to steel stirrups.
2- Using glass fiber and tensar wire mesh instead of steel stirrups exhibit high ultimate failure load with respect to control specimen.
3- Tensar (Polyethylene) wire mesh has high effect in increasing load capacity, deflection, the shear stresses and cracks propagate.
4- The cracks propagation and its number and width decreased by using glass fiber and tensar wire mesh especially in specimens with two and three layers of wire mesh.
5- There a reasonable agreement between experimental and numerical results obtained in form of ultimate failure load, deflection and shear stresses.
6- This work gives an acceptable prediction for shear stresses of box beams reinforced with glass fiber or tensar wire meshes where the obtained average ratio ($V_{u\ NLFEA}/V_{u\ EXP}$) was 0.938.

At the end, the composite either glass fiber or tensar wire mesh in reinforcement of box sections instead of steel stirrups has a good effect in failure load, deflection, cracks propagation and shear stresses.

REFERENCES

[1] ACI Committee 549. State of the art report on ferrocement. ACI 549-R97 manual of concrete practice, Detroit; 1997.

[2] ACI Committee 549-1R-88. Guide for design construction and repair of ferrocement. ACI 549-1R-88 and 1R-93 manual of concrete practice, Detroit; 1993.
[3] Logan, D. & Shah, S. P., Moment capacity and cracking behavior of ferrocement in flexure. ACI Journal Proceedings, 70 (12) (Dec. 1973) 799-804.
[4] Johnston, C. D. & Mowat, D. N., Ferrocement material behavior in flexure. Journal of the Structural Division, ASCE, 100, STIO, (Oct. 1974) 2053-69.
[5] Balaguru, P. N., Namaan, A. E. & Shah, S. P., Analysis and behavior of ferrocement in flexure. Journal of the Structural Division, ASCE, 103, STIO, (Oct. 1977) 1937-49.
[6] Huq, S. & Pama, R. P., Ferrocement in flexure–analysis and design. Journal of Ferrocement, 8 (3) (July 1988) 169-93.
[7] A1-Sulaimani, G. J. & Ahmad, S. F., Deflection and flexural rigidity of I- and box-beams. Journal of Ferrocement, 18, (Jan. 1988) 1-12.
[8] Al-Sulaimani, G. J., Ahmad, S. F. & Basunbul, 1. A., Study of the flexural strength of ferrocement 'flanged' beams. The Arabian Journal for Science and Engineering, 14 (1) (Jan. 1989) 33-46.
[9] Mansur, M. A. & Ong, K. C. G., Shear strength of ferrocement beams. American Concrete Institute Structural Journal, 84 (1) (Jan.-Feb. 1987) 10-17.
[10] El-Sayed, T.A. and Erfan, A.M., 2018. Improving shear strength of beams using ferrocement composite. Construction and Building Materials, 172, pp.608-617.
[11] E.C.P. 203/2018, 2018, Egyptian Code of Practice: Design and Construction for Reinforced Concrete Structures, Cairo, Egypt.
[12] ANSYS," Engineering Analysis system user's Manual" 2005, vol. 1&2, and theoretical manual. Revision 8.0, Swanson analysis system inc., Houston, Pennsylvania.